CNO abundances in the globular clusters NGC 1851 and NGC 6752[*]

David Yong,[1][†][‡] Frank Grundahl[2] and John E. Norris[1]

[1]*Research School of Astronomy and Astrophysics, Australian National University, Canberra ACT 2611, Australia*
[2]*Stellar Astrophysics Centre, Department of Physics and Astronomy, Aarhus University, Ny Munkegade 120, DK-8000 Aarhus C, Denmark*

ABSTRACT

We measure the C+N+O abundance sum in red giant stars in two Galactic globular clusters, NGC 1851 and NGC 6752. NGC 1851 has a split subgiant branch which could be due to different ages or C+N+O content while NGC 6752 is representative of the least complex globular clusters. For NGC 1851 and NGC 6752, we obtain average values of A(C+N+O) = 8.16 ± 0.10 (σ = 0.34) and 7.62 ± 0.02 (σ = 0.06), respectively. When taking into account the measurement errors, we find a constant C+N+O abundance sum in NGC 6752. The C+N+O abundance dispersion is only 0.06 dex, and such a result requires that the source of the light element abundance variations does not increase the C+N+O sum in this cluster. For NGC 1851, we confirm a large spread in C+N+O. In this cluster, the anomalous RGB has a higher C+N+O content than the canonical RGB by a factor of 4 (∼0.6 dex). This result lends further support to the idea that the two subgiant branches in NGC 1851 are roughly coeval, but with different CNO abundances.

Key words: Stars: abundances – Galaxy: abundances – globular clusters: individual: NGC 1851 – globular clusters: individual: NGC 6752.

1 INTRODUCTION

Galactic globular clusters continue to pose a series of intriguing questions concerning stellar evolution, stellar nucleosynthesis and chemical evolution. First, it has been known for several decades that globular clusters exhibit star-to-star variations in the CN and CH line strengths (e.g. Smith 1987). These molecular line strength variations are driven by star-to-star abundance variations for the light elements from C to Al (see reviews by Kraft 1994; Gratton, Sneden & Carretta 2004; Gratton et al. 2012a, for details.). Secondly, a star-to-star dispersion in iron-peak elements, and other elements, has long been known to exist in the globular cluster ω Centauri (e.g. Freeman & Rodgers 1975; Cohen 1981; Norris & Da Costa 1995; Smith et al. 2000; Johnson & Pilachowski 2010). More recently, abundance dispersions have also been identified in a number of globular clusters including M2 (Yong et al. 2014), M22 (Marino et al. 2009, 2011; Roederer, Marino & Sneden 2011), M54 (Carretta et al. 2010a), NGC 1851 (Yong & Grundahl 2008; Carretta et al. 2011), NGC 3201[1] (Simmerer et al. 2013), NGC 5824[2] (Da Costa, Held &

Saviane 2014) and Terzan 5 (Ferraro et al. 2009; Origlia et al. 2013), although the shape of the metallicity distribution function differs between these objects.

The light element abundance variations are believed to result from hydrogen burning at high temperature (Denisenkov & Denisenkova 1990; Langer, Hoffman & Sneden 1993; Prantzos, Charbonnel & Iliadis 2007). The astrophysical site in which these nuclear reactions occur continues to be debated with asymptotic giant branch (AGB) stars, fast rotating massive stars, massive binaries and supermassive stars among the candidates (Fenner et al. 2004; Ventura & D'Antona 2005; Karakas et al. 2006; Decressin et al. 2007b; de Mink et al. 2009; Marcolini et al. 2009; Denissenkov & Hartwick 2014). Additionally, many details regarding the production of these abundance variations including the initial mass function, minimum time-scale, required mass budget, degree of (or need for) dilution with pristine gas and star formation modes still need to be established (Bastian et al. 2013; Renzini 2013). An important constraint on the site and nature of the nucleosynthesis comes from the C+N+O[3] abundance sum. In fast rotating massive stars, the C+N+O abundance sum is expected to remain constant; the slow winds are enriched in H-burning products whereas the He-burning products are ejected at later times at high velocity (Decressin et al. 2007b; Decressin,

---

[1] Other studies of this cluster do not find evidence for an iron dispersion (Carretta et al. 2009; Muñoz, Geisler & Villanova 2013).

[2] This result is based on metallicities from the calcium triplet.

---

[3] Here and throughout the paper, 'C+N+O' is the sum of the C, N and O abundances and these values are on the log ϵ scale. For example, the Asplund et al. (2009) solar values are log ϵ(C) = 8.43, log ϵ(N) = 7.83 and log ϵ(O) = 8.69 and this gives C+N+O = 8.92.

Charbonnel & Meynet 2007a). AGB stars, on the other hand, are expected to increase the C+N+O abundance sum (Fenner et al. 2004). That said, adjustments to the input physics can result in AGB models that produce an essentially constant C+N+O abundance sum (Ventura & D'Antona 2005).

The dispersion in heavy element abundances in ω Cen has led to the suggestion that it is the nucleus of an accreted dwarf galaxy (Freeman 1993; Bekki & Freeman 2003). For the recently discovered globular clusters with dispersions in iron-peak elements, the chemical similarities with ω Centauri may also require a similarly complex formation process. The sequence of events leading to the formation of these globular clusters remains poorly understood. Some of these objects exhibit multiple subgiant branches, and it is well known that the C+N+O abundance sum plays a key role in age determinations based on subgiant branch analyses (Rood & Crocker 1985). In the case of NGC 1851, the double subgiant branch (Milone et al. 2008) could be composed of two coeval populations with different mixtures of C+N+O abundances (Cassisi et al. 2008). Since the discovery of the double subgiant branch in NGC 1851, understanding its nature and formation history has been an active area of research (D'Antona et al. 2009; Han et al. 2009; Lee et al. 2009; Milone et al. 2009; Olszewski et al. 2009; Ventura et al. 2009; Zoccali et al. 2009; Carretta et al. 2011, 2012; Bekki & Yong 2012; Gratton et al. 2012c, 2012b; Lardo et al. 2012; Joo & Lee 2013; Marino et al. 2014). Indeed, it has been suggested that NGC 1851 may be the product of the merger of two clusters (Carretta et al. 2010b).

Despite the importance of the C+N+O content in globular clusters, there is only a modest number of studies on this topic (e.g. Brown, Wallerstein & Oke 1991; Dickens et al. 1991; Ivans et al. 1999; Cohen & Meléndez 2005; Smith et al. 2005; Yong et al. 2008b; Marino et al. 2011, 2012; Dotter et al. 2014). For NGC 1851, there are conflicting results regarding the C+N+O abundance sum (Yong et al. 2009; Villanova, Geisler & Piotto 2010). In the case of NGC 6752, Carretta et al. (2005) found that the C+N+O abundance sum was constant, within a factor of $\sim$2, for their sample of dwarfs and subgiants. We note that the C, N and O abundances are typically derived from the CH molecular lines, CN molecular lines and [O I] atomic lines, respectively. Due to molecular equilibrium, deriving the C abundance requires knowledge of the O abundance, and vice versa. Similarly, N abundances derived from the CN lines require knowledge of both the C and O abundances. For N measurements from CN molecular lines, the uncertainties can be magnified by the errors associated with both the C and O abundances. The situation can be improved by the analysis of the NH molecular lines. One advantage is that the inferred N abundance requires no knowledge of the C and/or O abundances. A clear disadvantage is that the best NH molecular lines are near 3360 Å; this is a crowded spectral region and red giant branch stars have limited flux in the blue relative to redder wavelengths.

The purpose of this paper is to examine the C+N+O abundance sum in the globular clusters NGC 1851 and NGC 6752. NGC 6752 is representative of the least complex globular clusters; it has a single subgiant branch (when not viewed using filters sensitive to molecular lines of CH, CN, CO, NH and OH: Milone et al. 2013) and no large dispersion in iron-peak elements (modulo the small but statistically significant variations identified by Yong et al. 2013). Measurements of C+N+O in this cluster would serve to constrain the origin of the light element abundance variations in globular clusters and provide an important baseline for comparison with multiple subgiant branch clusters. NGC 1851 is representative of multiple subgiant branch globular clusters with star-to-star abundance dis-

persions for iron-peak and neutron-capture elements. Measurements of C+N+O in this cluster would help establish whether or not the double subgiant branch populations are coeval. The outline of the paper is as follows. Section 2 describes the sample selection and observations. The analysis is presented in Section 3. Section 4 includes the results and discussion and we present concluding remarks in Section 5.

2 SAMPLE SELECTION AND OBSERVATIONS

The targets were selected from the Strömgren *uvby* photometry from Grundahl et al. (1999) (see Fig. 1 and Tables 1 and 2). For NGC 6752, the targets were a subset of those observed by Grundahl et al. (2002) and lie near the RGB bump (see Table 1). For NGC 1851, the targets lie on the canonical RGB, the AGB and the anomalous RGB[4] (see Table 2). To avoid contamination from nearby stars, the targets were selected to have no neighbours within 2.5 arcsec and ΔVmag = 2.5. Based on their location in CMDs, stellar parameters and radial velocities, all stars are likely cluster members.

Observations of these targets were obtained using the multiobject spectrograph FLAMES/GIRAFFE (Pasquini et al. 2002) in IFU mode. The field of view is 25 arcmin and there are 15 IFU units each of which has an aperture of 2×3 arcsec^2 consisting of 20 square spaxels of length 0.52 arcsec. For NGC 1851, we obtained spectra using the HR4 ($R = 32\,500$:$\sim$4300 Å; total exposure time of 7.9 h), HR13 ($R = 36\,000$:$\sim$6300 Å, total exposure time of 1.4 h) and HR19B ($R = 35\,000$:$\sim$8000 Å, total exposure time of 1.3 h) gratings (see Fig. 2). For NGC 6752, we used the HR4 (total exposure time of 3.6 h) and HR19B (total exposure time of 1.3 h) gratings. A telluric standard was also observed using the HR13 and HR19 gratings.

For the purposes of this project, we decided that the higher spectral resolution provided by the IFU mode relative to the MEDUSA mode (e.g. $R_{\mathrm{IFU}} = 32\,500$ versus $R_{\mathrm{MEDUSA}} = 20\,350$ for HR4) was a major advantage for deriving accurate and precise chemical abundances in the program stars. Additionally, the smaller number of targets that can be observed in the IFU mode (up to 15) versus MEDUSA mode (up to 132) was not considered to be a disadvantage for this project. For NGC 6752, there were only some 21 objects for which we had already derived N and O abundances and measurements of C abundances in up to 15 of these targets would be sufficient to study the C+N+O sum, i.e. an additional 100 measurements of C in objects with no N and O measurements would be surplus to requirements. For NGC 1851, there were only seven anomalous RGB objects brighter than $V \simeq 14.8$ such that the 15 targets could include a reasonable number of anomalous RGB, canonical RGB and AGB stars. While our primary objective was to compare the canonical and anomalous RGBs, recent studies of AGB stars have indicated that they may be populated exclusively by Na-poor objects (Campbell et al. 2013). Furthermore, the RGB and AGB populations in NGC 1851 exhibit a complex distribution in CN molecular line strengths (Campbell et al. 2012). Therefore, we were also interested in studying the CNO content of AGB stars in NGC 1851.

For each program star, we examined the spectrum obtained from each spaxel. After testing various options, we summed the four

---

[4]In the various tables, the anomalous RGB objects are denoted by 'm1' since they were first noticed as unusually red in the CMDs involving the *m1* index in the Grundahl et al. (1999) photometry.
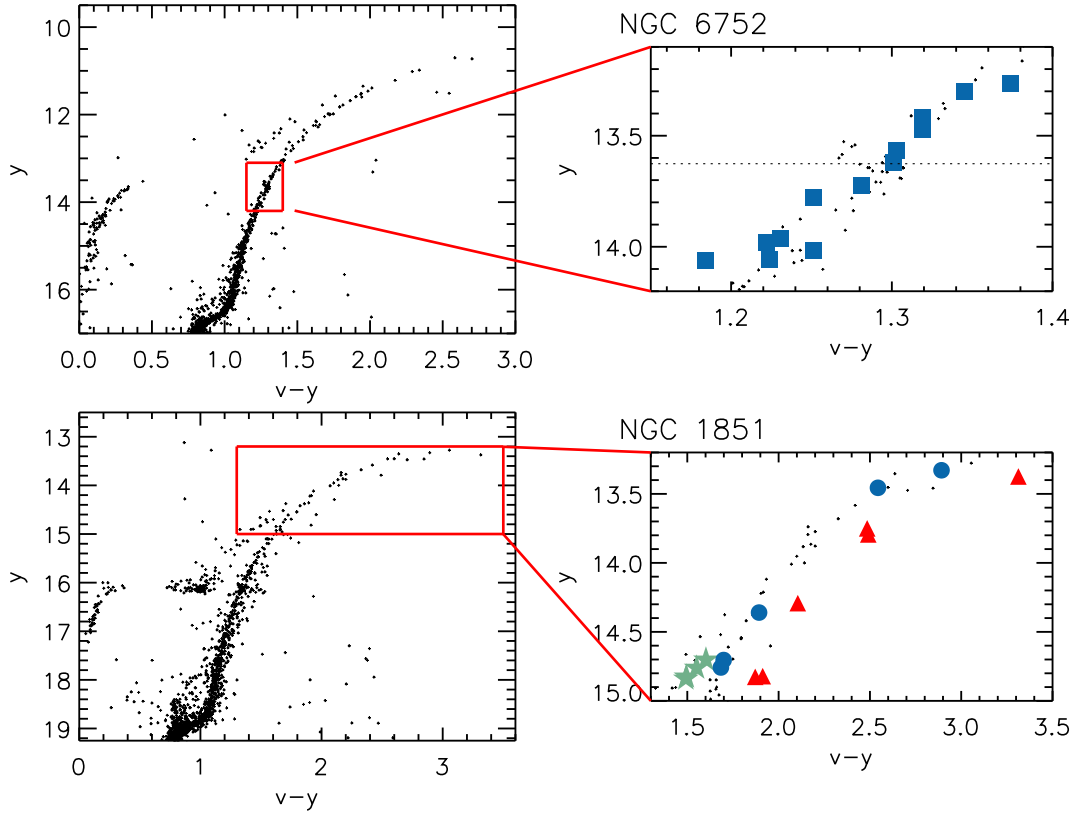
Figure 1. Colour–magnitude diagrams for y versus $v - y$ for NGC 6752 (upper) and NGC 1851 (lower) using photometry from Grundahl et al. (1999). The right hand panels show a smaller region of the CMD. For NGC 6752, the program stars are marked by large blue squares and the location of the RGB bump is indicated by the dotted line. For NGC 1851, the aqua star symbols, blue circles and red triangles refer to AGB, canonical RGB and anomalous RGB stars, respectively.

Table 1. Stellar parameters and CNO abundances for NGC 6752.

Name 1 (1)	Name 2[a] (2)	RA 2000 (3)	Dec. 2000 (4)	V (5)	T_{eff} (6)	$\log g$ (7)	ξ_t (8)	[Fe/H] (9)	C (10)	N_{NH} (11)	N_{CN} (12)	O (13)	C+N+O[b] (14)
NGC 6752-1	B2882	19 10 47	−60 00 43	13.27	4749	1.95	1.41	−1.58	6.41	6.36	<7.36	7.60	7.65
NGC 6752-2	B1635	19 11 11	−60 00 17	13.30	4779	2.00	1.39	−1.59	6.06	7.55	7.95	6.93	7.65
NGC 6752-4	B611	19 11 33	−60 00 02	13.42	4806	2.04	1.40	−1.61	6.16	7.35	7.85	6.96	7.52
NGC 6752-6	B3490	19 10 34	−59 59 55	13.47	4804	2.06	1.40	−1.61	6.36	7.30	7.60	7.10	7.54
NGC 6752-8	B3103	19 10 45	−59 58 18	13.56	4910	2.15	1.33	−1.62	6.51	6.25	<7.25	7.61	7.66
NGC 6752-9	B3880	19 10 26	−59 59 05	13.57	4824	2.11	1.38	−1.63	6.61	6.05	<7.05	7.64	7.69
NGC 6752-11	B2728	19 10 50	−60 02 25	13.62	4829	2.13	1.32	−1.64	6.41	7.15	7.65	7.36	7.60
NGC 6752-15	B2782	19 10 49	−60 01 55	13.73	4850	2.19	1.35	−1.61	6.56	5.70	<7.20	7.70	7.73
NGC 6752-16	B4446	19 10 15	−59 59 14	13.78	4906	2.24	1.32	−1.60	6.41	7.40	7.70	7.08	7.60
NGC 6752-19	B1113	19 11 23	−59 59 40	13.96	4928	2.32	1.29	−1.61	6.56	6.90	7.45	7.32	7.51
NGC 6752-20	...	19 10 36	−59 56 08	13.98	4929	2.33	1.32	−1.59	6.15	7.45	7.90	7.12	7.63
NGC 6752-21	...	19 11 13	−60 02 30	14.02	4904	2.33	1.29	−1.61	6.51	6.95	7.45	7.51	7.65
NGC 6752-23	B1668	19 11 12	−59 58 29	14.06	4916	2.35	1.27	−1.62	6.16	7.45	7.95	7.15	7.64
NGC 6752-24	...	19 10 44	−59 59 41	14.06	4948	2.37	1.15	−1.65	6.51	5.95	<7.45	7.53	7.58

Notes: [a]Star names from Buonanno et al. (1986).
[b]N is from NH.

central spaxels (8, 9, 12 and 13) for a given star in a given observing block. In all cases, these four spaxels contained the vast majority of the flux. To produce the final spectrum for a program star, the spectra from multiple observing blocks were combined. Note that star NGC 1851 NR 5246 is affected by TiO and we do not present chemical abundances for this object.

Heliocentric radial velocities for the NGC 1851 stars are presented in Table 3. These values were determined by comparing the observed and rest wavelengths for about 80 atomic lines in each program star. We find an average value of $+320.2 \pm 1.3$ km s^{-1} ($\sigma = 4.8$ km s^{-1}) which agrees with values from the literature: $+320.5 \pm 0.6$ km s^{-1} (Harris 1996, updated in 2010) $+320.26$ km s^{-1} (rms $= 3.74$ km s^{-1}) (Carretta et al. 2011); $+320.0 \pm 0.4$ km s^{-1} (Scarpa et al. 2011); $+318.2 \pm 0.5$ km s^{-1} (Gratton et al. 2012c); $+319.5 \pm 0.5$ km s^{-1} (Marino et al. 2014). That is, all program stars are likely cluster members.

Table 2. Stellar parameters and CNO abundances for NGC 1851.

Name 1 (1)	Name 2[a] (2)	RA 2000 (3)	Dec. 2000 (4)	V (5)	CMD (6)	T_{eff} (7)	log g (8)	ξ_t (9)	[Fe/H] (10)	C (11)	N[b] (12)	O (13)	C+N+O (14)
NR 712	236	05 13 59.45	−40 05 22.59	14.70	RGB	4392	1.42	1.50	−1.33	6.26	6.76	7.73	7.79
NR 1290	168	05 14 19.34	−40 04 23.85	13.33	RGB	3738	0.27	1.95	−1.26	6.26	7.96	7.83	8.21
NR 4740	126	05 14 17.24	−40 02 08.01	14.36	RGB	4259	1.19	1.50	−1.20	6.31	7.11	7.73	7.84
NR 6221	...	05 14 07.78	−40 01 18.15	14.76	RGB	4426	1.46	1.40	−1.27	6.11	7.75	7.33	7.63
NR 6250	...	05 14 02.80	−40 01 22.78	13.46	RGB	3924	0.54	1.85	−1.30	6.16	7.81	7.68	8.06
NR 1469	210	05 14 10.35	−40 04 23.57	14.76	AGB	4639	1.54	1.80	−1.32	6.21	8.16	...	...
NR 2352	...	05 14 13.52	−40 03 40.88	14.84	AGB	4688	1.60	1.40	−1.16	6.16	8.06	...	...
NR 3272	137	05 14 15.02	−40 03 04.08	14.83	AGB	4607	1.54	1.65	−1.33	6.11	7.66	7.93	8.12
NR 8066	22	05 14 10.35	−39 58 14.83	14.70	AGB	4596	1.49	1.70	−1.32	6.16	8.11	7.53	8.22
NR 2953	...	05 14 05.86	−40 03 24.57	13.75	m1	3958	0.70	1.95	−1.21	5.86	8.81	7.13	8.82
NR 3213	112	05 14 25.96	−40 02 53.78	13.79	m1	4002	0.76	2.20	−1.30	6.21	8.46	7.33	8.49
NR 5171	...	05 14 06.60	−40 02 02.63	14.83	m1	4315	1.42	1.55	−1.34	6.26	8.16	7.28	8.22
NR 5246	...	05 14 01.33	−40 02 05.81	13.37	m1	3666	0.18		*Spectrum affected by TiO*				
NR 5543	319	05 13 50.30	−40 02 06.98	14.82	m1	4402	1.47	1.70	−1.30	6.46	8.21	...	...
NR 6217	58	05 14 14.47	−40 01 10.93	14.29	m1	4212	1.13	1.70	−1.26	6.06	8.36	7.28	8.40

Notes: [a]Star names from Stetson (1981).
[b] The N abundances are from CN and have been adjusted by −0.44 dex (see Sections 4.1 and 4.2 for details).
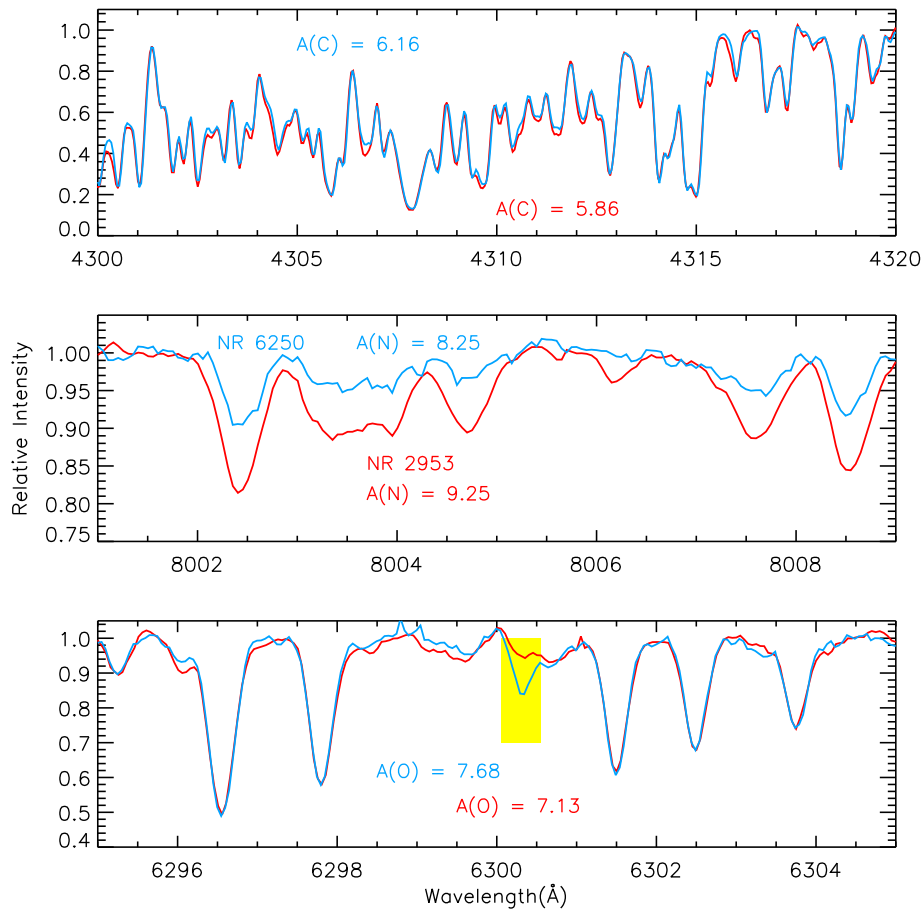

Figure 2. A portion of the spectra for two stars in NGC 1851 with similar stellar parameters, but belonging to the two different RGBs. NR 6250 (blue) is a canonical RGB star while NR 2953 (red) is an anomalous RGB star. The upper and middle panels include regions used in determining the C and N abundances, respectively. In the lower panel, the 6300 Å [O I] line is highlighted. The C, N and O abundances for both stars are included in the panels.

Table 3. Heliocentric radial velocities for NGC 1851.

Name (1)	CMD (2)	RV (km s^{-1}) (3)	σRV (km s^{-1}) (4)
NR 712	RGB	+315.4	0.5
NR 1290	RGB	+327.5	0.6
NR 4740	RGB	+317.6	0.5
NR 6221	RGB	+316.8	0.8
NR 6250	RGB	+322.6	0.7
NR 1469	AGB	+313.3	0.8
NR 2352	AGB	+314.4	0.9
NR 3272	AGB	+326.4	0.7
NR 8066	AGB	+326.3	0.7
NR 2953	m1	+324.5	0.8
NR 3213	m1	+321.8	0.7
NR 5171	m1	+315.4	0.9
NR 5246	m1	...	...
NR 5543	m1	+320.7	0.9
NR 6217	m1	+321.6	0.8

3 ANALYSIS

We commenced our analysis using one-dimensional wavelength-calibrated pipeline reduced spectra. The signal-to-noise ratio exceeded 100 per pixel for each wavelength setting in all program stars. The spectra were normalized by fitting low-order polynomial functions. For the HR19B spectra (~8000 Å), we divided the program stars by the telluric standard.

In the case of NGC 6752, stellar parameters for all program stars have been obtained from our previous studies (Grundahl et al. 2002; Yong et al. 2003). In the case of NGC 1851, we derived stellar parameters in the following manner (the approach is very similar, but not identical, to that applied to NGC 6752). The effective temperature, $T_{\rm eff}$, was determined using colour–temperature relations (Alonso, Arribas & Martínez-Roger 1999; Ramírez & Meléndez 2005) based on the infrared flux method. We used the Strömgren photometry from Grundahl et al. (1999) and *JHK* photometry from 2MASS (Skrutskie et al. 2006) and adopted a reddening of $E(B-V) = 0.02$ from the 2010 version of the Harris (1996) catalogue. For each star we obtained values for $T_{\rm eff}$ from the two calibrations, Alonso et al. (1999) and Ramírez & Meléndez (2005), using the $b-y$, $V-J$, $V-H$ and $V-K$ colours (with appropriate transformations from 2MASS to the *TCS* system using the relations in Alonso, Arribas & Martinez-Roger 1994; Carpenter 2001). We adopted the average $T_{\rm eff}$, weighted by the uncertainties for each colour, and note that the mean difference, Alonso et al. − Ramírez & Meléndez, is +55 K ± 17 K ($\sigma = 64$ K). The surface gravity, log g, was determined using $T_{\rm eff}$, a distance modulus $(m-M)_V = 15.47$ (Harris 1996), bolometric corrections from Alonso et al. (1999) and a mass of 0.8 M$_\odot$ for the RGB objects and 0.7 M$_\odot$ for the AGB stars. Observational constraints on the masses of RGB stars in globular clusters can be obtained from eclipsing binaries near the main-sequence turnoff. In the comparable age and metallicity globular clusters 47 Tuc and M4, masses of ~0.8 M$_\odot$ are obtained by Thompson et al. (2010) and Kaluzny et al. (2013), respectively. AGB stars in globular clusters do not have observational constraints on their masses, and these values are subject to additional uncertainties including mass loss. Dotter (2008) estimate that horizontal branch stars, i.e. the evolutionary phase prior to the AGB, have lost ~0.15 M$_\odot$, while Gratton et al. (2010) estimate a value of ~0.20 M$_\odot$. Therefore, our assumption of 0.70 M$_\odot$ on the AGB may be slightly overestimated.

Table 4. Line list for the NGC 1851 stars.

Wavelength Å (1)	Species^a (2)	L.E.P. (eV) (3)	log gf (4)	NR 712 (mÅ) (5)	Source^b (6)
6154.23	11.0	2.10	−1.57	11.6	A
6160.75	11.0	2.10	−1.26	18.7	A
6318.71	12.0	5.11	−1.94	25.3	A
6319.24	12.0	5.11	−2.16	...	A
6120.24	26.0	0.91	−5.97	19.0	B
6136.62	26.0	2.45	−1.40	...	B
6151.62	26.0	2.18	−3.30	66.7	A

Notes: ^{a}The digits to the left of the decimal point are the atomic number. The digit to the right of the decimal point is the ionization state ('0' = neutral, '1' = singly ionized).
^{b}A = Gratton et al. (2003); B = Oxford group including Blackwell et al. (1979a, 1980, 1986), Blackwell, Petford & Shallis (1979b), and Blackwell, Lynas-Gray & Smith (1995).
This table is published in its entirety in the electronic edition of the paper. A portion is shown here for guidance regarding its form and content.

We then measured equivalent widths (EWs) for a set of lines using IRAF^5 and DAOSPEC (Stetson & Pancino 2008). The line list is presented in Table 4. With estimates for $T_{\rm eff}$ and log g we generated one-dimensional local thermodynamic equilibrium (LTE) model atmospheres with [α/Fe] = +0.4 from the Castelli & Kurucz (2003) grid using the interpolation software tested in Allende Prieto et al. (2004). Chemical abundances were computed using the LTE stellar line analysis program MOOG (Sneden 1973; Sobeck et al. 2011). The microturbulent velocity, ξ_t, was obtained by forcing no trend between the abundance from Fe I and the reduced equivalent width, log (EW/λ). The average number of Fe I and Fe II lines measured in a given star was 29 and 3, respectively. Following Yong et al. (2005), we estimate that the internal uncertainties in $T_{\rm eff}$, log g and ξ_t are 30 K, 0.1 dex and 0.1 km s^{-1}, respectively, for NGC 6752. For NGC 1851, the uncertainty in $T_{\rm eff}$ can be obtained by the weighted error from the colour–temperature relations. This value is 32 K, and we conservatively adopt 40 K as the uncertainty. For the surface gravity, uncertainties in the temperature, distance, reddening, $T_{\rm eff}$ and V mag when added in quadrature translate into an error in log g of 0.05 dex, and we conservatively adopt an error of 0.1 dex. For ξ_t, we plotted this quantity versus log g and fitted a straight line to the data. The scatter about the linear fit was 0.17 km s^{-1}, and a similar approach with respect to $T_{\rm eff}$ resulted in a scatter of 0.18 km s^{-1}. Thus, we adopt an uncertainty in ξ_t of 0.2 km s^{-1}.

Carbon abundances were obtained by comparing synthetic with observed spectra in the vicinity of the 4300 Å CH molecular lines. We used the CH line list compiled by Plez et al. (2009, private communication). In our analysis, the dissociation energy for CH was 3.465 eV.

Although nitrogen abundances had already been obtained in NGC 6752 based on the 3360 Å NH molecular lines (Yong et al. 2008a), we re-measured these values using the Sobeck et al. (2011) version of MOOG. The average difference (2008 values minus updated values) is +0.09 dex ± 0.01 dex ($\sigma = 0.05$ dex). We also measured nitrogen from the 8000 Å CN molecular lines using the line list from Reddy et al. (2002). The dissociation energy for CN was 7.750 eV. (When

---

^{5}IRAF is distributed by the National Optical Astronomy Observatories, which are operated by the Association of Universities for Research in Astronomy, Inc., under cooperative agreement with the National Science Foundation.

using a CN line list kindly provided by M. Asplund, essentially identical N abundances were obtained.)

Oxygen abundances were determined by comparing synthetic and observed spectra near the 6300 Å [O I] line. In NGC 1851, relative abundances for Na, Mg and Zr were measured based on an equivalent-width analysis. The Asplund et al. (2009) solar abundances were adopted and the chemical abundances are presented in Tables 1, 2 and 5. The metallicity, [Fe/H], was determined by averaging the results from Fe I and Fe II weighted by the number of lines from each species (this approach strongly favours Fe I).

As noted in the Introduction, the abundances for C, N and O are coupled due to molecular equilibrium. The processes described above required iteration until self-consistent abundances were obtained for a given program star. In the upper panel of Fig. 2, the star with the lower C abundance (NR 2953) has stronger CH lines relative to the star with the higher C abundance (NR 6250). This apparently unusual situation is a direct consequence of the relative O abundances (NR 6250 has a considerably higher abundance) and molecular equilibrium.

Uncertainties in the abundance ratios were obtained in the following manner. We repeated the analysis and varied the stellar parameters, one at a time, by their uncertainties. We also considered the uncertainty in the metallicity used to generate the model atmosphere, [m/H], and varied this value by 0.1 dex. The systematic uncertainty was obtained by adding these four error terms, in quadrature (although we note that this approach ignores covariances). To obtain the total error, we added the systematic and random errors in quadrature. Due to molecular equilibrium, the uncertainty in the O abundance affects the derived C abundance, and vice versa. For these two species, we include an additional error term accounting for the uncertainty in these abundances. For the N abundances derived from the CN molecular lines, we also need to take into account the uncertainties in the C and O abundances. The uncertainty in the O abundance produces the dominant term in the error budget for N as derived from CN lines. For these CNO abundances derived from fitting synthetic spectra, we adopted a fitting error based on χ^2 analysis (i.e. the value for which $\Delta\chi^2 = 1$) and use these values as the random error. The errors are presented in Table 6.

For NGC 1851, a subset of our program stars were studied in Carretta et al. (2010b), Carretta et al. (2011) and Villanova et al. (2010). We defer our comparison with the latter until Section 4.2. For the seven stars in common with Carretta et al. (2010b, 2011), we find the following differences in the sense 'this study − Carretta et al.': $\Delta RV = +0.8 \pm 0.3$ km s^{-1}; $\Delta T_{eff} = -10 \pm 14$ K; $\Delta\log g = -0.05 \pm 0.01$ cgs; $\Delta\xi_t = +0.20 \pm 0.14$ km s^{-1}; Δ[Fe/H] $= -0.14 \pm 0.03$ dex; Δ[O/Fe] $= +0.11 \pm 0.16$ dex; Δ[Na/Fe] $= -0.15 \pm 0.06$ dex; Δ[Mg/Fe] $= -0.04 \pm 0.05$ dex; Δ[Zr/Fe] $= -0.03 \pm 0.09$ dex. Overall, our radial velocities, stellar parameters and chemical abundances are in good agreement.

4 RESULTS AND DISCUSSION

4.1 NGC 6752

In Fig. 3, we plot the C+N+O distribution for NGC 6752. In the upper panel, the N abundances are derived from the analysis of the NH lines. The mean C+N+O abundance is 7.62 ± 0.02 dex and the standard deviation of the C+N+O distribution is $\sigma = 0.06 \pm 0.01$ dex. In order to understand whether this abundance dispersion is consistent with a constant C+N+O value convolved with the measurement uncertainty, we conducted the following test. For a representative star, we replaced the C abundance by a random
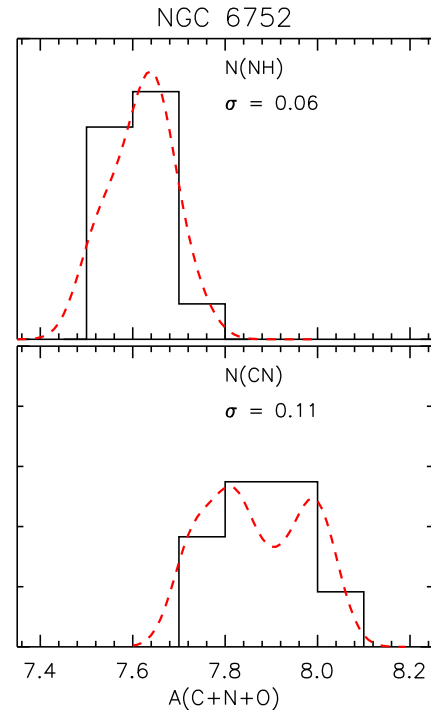

Figure 3. The distribution of the C+N+O abundance sum in NGC 6752 (the black histogram has a bin width of 0.1 dex). The red dashed line is a generalized histogram (Gaussian kernel $\sigma = 0.10$ dex). In the upper panel, the N abundances are from the analysis of the NH lines. In the lower panel, the N abundances are from the analysis of the CN lines.

number drawn from a normal distribution of width 0.07 dex (i.e. the measurement uncertainty for C), centred at the $\log\epsilon$ (C) value. A similar approach was taken to replace the N and O abundances, and we note that their measurement uncertainties are 0.09 and 0.06 dex, respectively. This produces a new set of C+N+O abundances. We repeated the process for 10^6 realizations and measured the standard deviation of the C+N+O distribution. As expected, when considering a star whose C+N+O sum is dominated by N, the standard deviation of the C+N+O distribution is 0.08 dex, and this value is essentially the uncertainty in N, 0.09 dex. Similarly, for a star whose C+N+O sum is dominated by O, the standard deviation of the C+N+O distribution is 0.05 dex, and this is comparable to the uncertainty in O, 0.06 dex. Therefore, we argue that our C+N+O distribution is consistent with a single value convolved with the measurement errors.

In the lower panel of Fig. 3, we again plot the C+N+O distribution but with N abundances derived from the analysis of the CN lines. In this case, the mean C+N+O abundance is 7.87 ± 0.04 dex and the standard deviation of the C+N+O distribution is $\sigma = 0.11 \pm 0.03$ dex. To understand whether the abundance dispersion is consistent with a constant value of C+N+O convolved with the measurement uncertainty, we adopted the same approach described above but with the uncertainty in N of 0.10 dex as appropriate for the CN analysis. As before, we find that the C+N+O distribution is consistent with a single value when taking into account the measurement errors. Therefore, the first main conclusion we draw is that the C+N+O abundance sum in NGC 6752 is constant. While a similar conclusion was reached by Carretta et al. (2005), in this work we achieve higher precision; our errors in the C+N+O sum are at or below the 0.10 dex level.

Table 5. Na, Mg and Zr abundances for NGC 1851.

Name	CMD	A(Na)	A(Mg)	A(Zr)	[Na$_{NLTE}$/Fe]^a	[Mg/Fe]	[Zr/Fe]
(1)	(2)	(3)	(4)	(5)	(6)	(7)	(8)
NR 712	RGB	4.79	6.57	1.35	−0.18	0.30	0.10
NR 1290	RGB	4.99	6.63	1.38	−0.04	0.29	0.07
NR 4740	RGB	4.78	6.60	1.33	−0.31	0.20	−0.05
NR 6221	RGB	5.01	6.59	1.49	−0.02	0.26	0.18
NR 6250	RGB	5.06	6.55	1.37	0.07	0.25	0.09
NR 1469	AGB	5.35	6.56	<1.73	0.35	0.28	<0.47
NR 2352	AGB	5.34	6.70	<1.83	0.18	0.26	<0.41
NR 3272	AGB	5.04	6.43	<1.67	0.06	0.16	<0.42
NR 8066	AGB	5.38	6.51	<1.66	0.39	0.22	<0.40
NR 2953	m1	5.74	6.75	1.61	0.60	0.36	0.23
NR 3213	m1	5.73	6.74	1.81	0.70	0.44	0.53
NR 5171	m1	5.34	6.61	1.51	0.37	0.35	0.27
NR 5246	m1	...	...	...	...	...	...
NR 5543	m1	5.47	6.70	1.59	0.46	0.40	0.31
NR 6217	m1	5.46	6.73	1.45	0.41	0.39	0.13

Note: ^{a}Non-LTE corrections from Lind et al. (2011).

Table 6. Abundance errors from uncertainties in atmospheric parameters and element abundances.

Name	C	N$_{NH}$	N$_{CN}$	O	Na	Mg	Zr	Fe
(1)	(2)	(3)	(4)	(5)	(6)	(7)	(8)	(9)
			NGC 6752-11					
T_{eff} + 30 K	−0.03	−0.04	−0.05	−0.01	...	...	...	...
log g + 0.1 dex	0.01	0.04	0.00	−0.04	...	...	...	...
ξ_t + 0.1 km s^{-1}	0.02	0.04	0.01	0.00	...	...	...	...
[m/H] + 0.1 dex	−0.04	−0.03	−0.05	−0.03	...	...	...	...
A(O) + 0.05 dex	−0.01	...	0.07	...	...	...	...	...
A(C) + 0.06 dex	...	...	−0.01	0.00	...	...	...	...
Random error^a	0.04	0.05	0.03	0.03	...	...	...	...
Total	0.07	0.09	0.10	0.06	...	...	...	...
			NGC 1851 NR 4740 (RGB)					
T_{eff} + 40 K	−0.04	...	0.03	0.01	−0.04	−0.01	−0.09	−0.02
log g + 0.1 dex	−0.04	...	−0.04	−0.04	0.01	0.00	0.00	−0.03
ξ_t + 0.2 km s^{-1}	−0.02	...	0.01	0.02	0.02	0.02	0.01	0.06
[m/H] + 0.1 dex	−0.07	...	−0.03	−0.02	0.00	0.00	0.00	−0.01
A(O) + 0.05 dex	−0.04	...	0.10	...	...	...	...	...
A(C) + 0.09 dex	...	...	−0.04	−0.02	...	...	...	...
Random error	0.04	...	0.03	0.03	0.04	0.05	0.04	0.04
Total	0.11	...	0.13	0.06	0.06	0.06	0.10	0.08
			NGC 1851 NR 6217 (m1)					
T_{eff} + 40 K	−0.01	...	0.05	0.01	−0.03	0.01	−0.08	0.01
log g + 0.1 dex	−0.01	...	−0.08	−0.05	0.00	0.00	0.00	−0.03
ξ_t + 0.2 km s^{-1}	0.02	...	0.02	0.01	0.04	0.02	0.02	0.05
[m/H] + 0.1 dex	−0.11	...	−0.06	−0.01	0.01	0.00	0.00	−0.01
A(O) + 0.05 dex	−0.02	...	0.18	...	...	...	...	...
A(C) + 0.11 dex	...	...	−0.05	0.01	...	...	...	...
Random error	0.04	...	0.03	0.04	0.06	0.05	0.06	0.05
Total	0.12	...	0.22	0.07	0.08	0.05	0.10	0.08

Note: ^{a}For C, N and O, this is the fitting error based on χ^2 analysis. For other elements, this is the standard error of the mean.

It is also evident that there is a systematic difference in the N abundance derived from the different molecular lines, NH versus CN. In Fig. 4, we plot the N abundance difference and note that the N abundance as derived from the CN molecular lines exceeds the values from the NH molecular lines by an average of 0.44 dex ($\sigma = 0.09$ dex). While the difference in N abundance directly affects the C+N+O abundance sum, the reason for this zero-point offset is not obvious. In their study of metal-poor giant stars, Spite et al. (2005) measured N abundances using the 3360 Å NH lines and the 3890 Å CN lines and found a 0.4 dex offset. In their case, the N abundances from NH exceeded those from CN. They attributed the abundance differences to uncertainties in the line positions, gf values and dissociation energy, and it is likely that a similar explanation applies to the N abundance offset in this study.
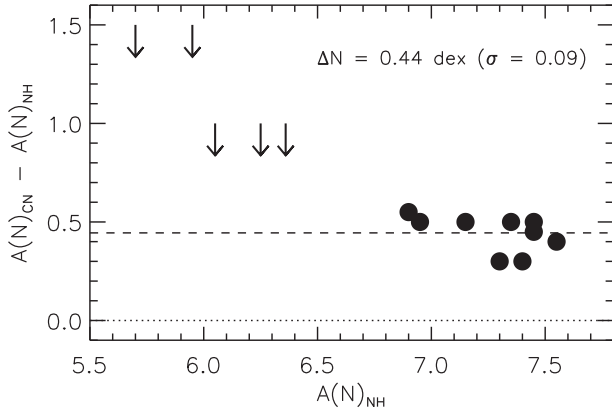
Figure 4. The difference in N abundance from the CN and NH molecular lines versus N abundance (NH) in NGC 6752.

We adopt the N abundance as derived from NH since this quantity has no dependence on the C and O abundances.

In light of the systematic difference in N abundance, we may ask the following question: if we expect that the C+N+O abundance sum should be constant, what would be the systematic shift in N abundances (as derived from NH) that produces the smallest abundance dispersion for C+N+O? The answer is a shift of +0.08 dex. When such an arbitrary shift is made, the resulting C+N+O abundance dispersion is essentially identical to our 0.06 dex value. The systematic N abundance differences underscore the importance of zero-point offsets when determining abundance sums such as C+N+O.

The program stars were selected by Grundahl et al. (2002) to lie above and below the RGB bump, $V = 13.626$ (Nataf et al. 2013). When adopting the N abundances from NH, the average C+N+O values for stars brighter and fainter than the RGB bump are identical, 7.62 ± 0.03 ($\sigma = 0.07$).

4.2 NGC 1851

We commence by noting that the N abundances in NGC 1851 were derived from the analysis of the CN lines. Recall that for NGC 6752, there was a 0.44 dex systematic offset between the N abundances from NH and CN. We adopted the NH values for NGC 6752. Therefore, when computing the C+N+O abundance sum for NGC 1851, we adjust the N abundances by -0.44 dex to place the two clusters on the same scale.[6]

In Fig. 5, we plot the C+N+O abundance distribution for NGC 1851. The mean C+N+O abundance is 8.16 ± 0.10 dex and the C+N+O abundance distribution is broad; the standard deviation is $\sigma = 0.34 \pm 0.08$ dex and the values span more than a factor of 10. To understand whether the observed abundance distribution is consistent with no intrinsic abundance dispersion, we adopted the same approach as for NGC 6752. For a representative canonical RGB star, our C, N and O uncertainties are 0.11, 0.13 and 0.06 dex, respectively. For a given canonical RGB star, we updated each of the C, N and O abundances by drawing random numbers from normal distributions of widths corresponding to the appropriate uncertainties and generated new C+N+O abundances. We repeated the process for 10^6 realizations and measured the standard deviation

---

[6]We are assuming that the offset inferred from NGC 6752 is applicable to NGC 1851. Clearly it would be of interest to measure N from NH in NGC 1851.
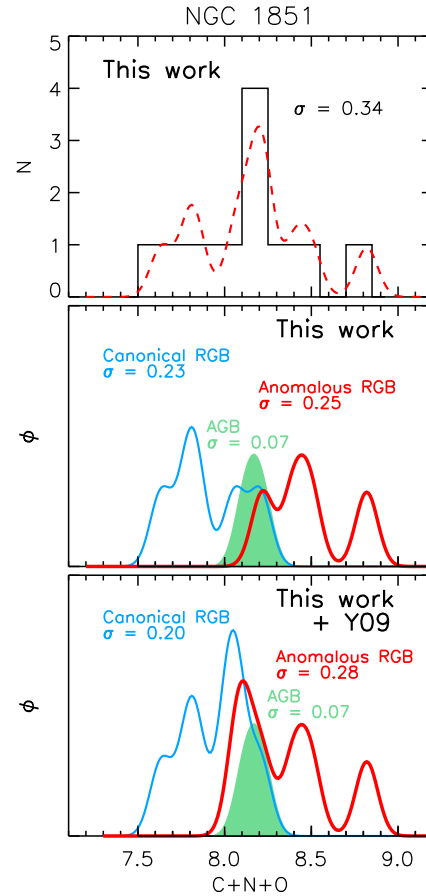

Figure 5. The distribution of the C+N+O abundance sum in NGC 1851 (the black histogram has a bin width of 0.15 dex). The red dashed line is a generalized histogram (Gaussian kernel $\sigma = 0.15$ dex). In the middle panel, generalized histograms are presented for the canonical RGB (five stars), anomalous RGB (four stars) and the AGB (two stars). The lower panel includes data from Yong et al. (2009).

of the C+N+O distribution. For the five canonical RGB objects, the standard deviations ranged from 0.06 to 0.10 dex, and as in the case of NGC 6752, these values depend on whether the CNO content is dominated by N or O. We repeated the process for the anomalous RGB objects noting that for a representative star, the C, N and O uncertainties are 0.12, 0.22 and 0.06 dex, respectively. For the four anomalous RGB objects, the standard deviations of the C+N+O distribution (based on 10^6 realizations) ranged from 0.19 to 0.21 dex (and we note that for all stars N dominates the C+N+O sum). In light of this error analysis, the C+N+O abundance distribution ($\sigma = 0.34 \pm 0.08$ dex) plotted in the upper panel of Fig. 5 appears to be inconsistent with a single C+N+O value convolved with measurement uncertainties ($\lesssim 0.20$ dex).

In the middle panel of Fig. 5, we plot the C+N+O distributions for the canonical RGB, AGB and anomalous RGB populations. The mean C+N+O abundances for each of the canonical and anomalous RGB populations are 7.90 ± 0.10 dex ($\sigma = 0.23 \pm 0.08$ dex) and 8.48 ± 0.13 dex ($\sigma = 0.25 \pm 0.09$ dex), respectively. We therefore confirm differences in CNO content between the canonical and anomalous RGB samples in NGC 1851, and this is the second main result in this paper.

Setting aside the two AGB stars, the canonical and anomalous RGB populations exhibit standard deviations for C+N+O of $\sigma = 0.23 \pm 0.08$ and $\sigma = 0.25 \pm 0.09$ dex, respectively. In the case

of the canonical RGB sample, the distribution is broader than that expected from measurement uncertainties alone ($\lesssim 0.10$ dex) and therefore indicates that there may be an intrinsic C+N+O spread within the canonical RGB population. For comparison, recall that in NGC 6752 (for both the CN and NH analyses), the C+N+O distribution exhibited no evidence for an intrinsic abundance spread given the measurement uncertainty (≤ 0.11 dex). In the case of the anomalous RGB sample in NGC 1851, the C+N+O distribution may be consistent with a constant value combined with the measurement uncertainties (~ 0.20 dex). We emphasize, however, that our sample sizes for both the canonical and anomalous RGBs are small, and therefore larger samples are needed to explore whether or not each population hosts an intrinsic spread in C+N+O. We also note that Carretta et al. (2014) found that the anomalous RGB is populated almost exclusively by N-rich stars. Within our limited sample, the anomalous RGB objects are all more N rich with respect to the canonical RGB.

We previously published C+N+O values for four stars in NGC 1851 (Yong et al. 2009) using the same spectral features as in this study. In the lower panel of Fig. 5, we combine those values with the current work (shifting the N abundances by -0.44 dex to be consistent with this study). Inclusion of those four stars (two in each of the canonical and anomalous RGBs) does not change the two key results, namely, that the mean C+N+O abundance is higher for the anomalous RGB (8.35 ± 0.11 dex) compared to the canonical RGB (7.94 ± 0.07 dex) and that the dispersion in C+N+O for the canonical RGB ($\sigma = 0.28 \pm 0.09$ dex) likely exceeds that expected from the measurement uncertainties. The dispersion for the anomalous RGB, $\sigma = 0.20 \pm 0.06$ dex, can be attributed to the measurement uncertainties.

Had we not applied the 0.44 dex shift to the N abundances, the canonical RGB would still have lower C+N+O compared to the anomalous RGB. Regardless of whether we include the Yong et al. (2009) sample or apply an abundance correction to N, in all cases the anomalous RGB has a higher content of C+N+O compared to the canonical RGB. Such a result supports the scenario proposed by Cassisi et al. (2008) in which the two subgiant branch populations are roughly coeval, but with different C+N+O abundances.

On the other hand, Villanova et al. (2010) reported constant C+N+O abundances for a sample of 15 red giants in NGC 1851. Their sample consisted of eight and seven stars on the canonical and anomalous RGBs, respectively. They used the same diagnostics to measure the CNO abundances as in this study and obtained C+N+O values of 7.99 ± 0.02 ($\sigma = 0.07$) and 8.02 ± 0.04 ($\sigma = 0.11$) for the canonical and anomalous RGBs, respectively. For comparison, our values for the canonical and anomalous RGBs are 7.90 ± 0.10 and 8.48 ± 0.13 dex, respectively. For the canonical RGB, our C+N+O values are in agreement. For the anomalous RGB, our C+N+O values disagree by ~ 0.45 dex.

There are three stars in common between this study and Villanova et al. (2010): NR 3213 = ID 9; NR 5543 = ID 16; NR 6217 = ID 20. For quantities published by both studies, we examine the differences in the sense 'this study − Villanova et al.' (while [Fe/H] can be compared for all three stars, we only measured O and C+N+O for the latter two objects) and find the following: Δ[Fe/H] $= -0.05 \pm 0.02$; ΔA(O) $= -0.04 \pm 0.08$; ΔC+N+O $= +0.42 \pm 0.10$ dex. We are unable to compare stellar parameters (T_{eff}, log g, ξ_t), radial velocities or individual C and N abundances since Villanova et al. (2010) did not publish these values. Nevertheless, there is good agreement for [Fe/H] and A(O). The stars in common are N-rich, so the C+N+O differences between this work and their study are likely due to differences in N abundance.
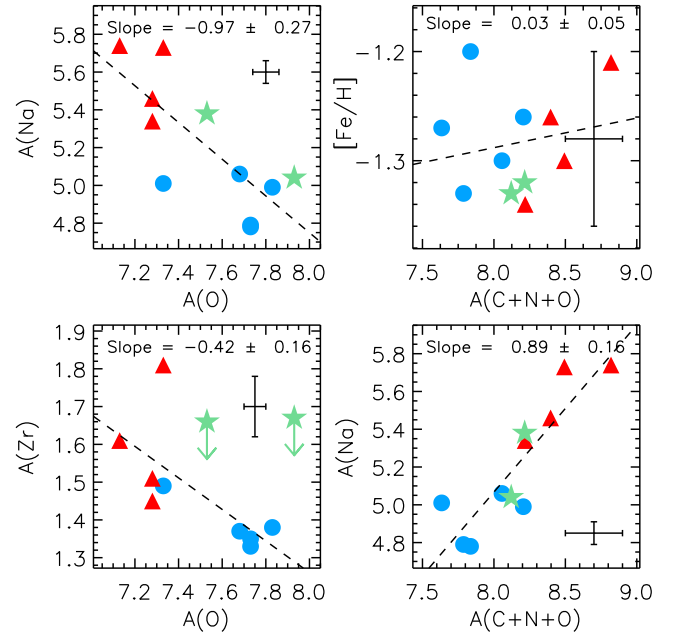

Figure 6. Abundance ratios for combinations of the light elements (C, N, O, Na), Fe and Zr in NGC 1851. The dashed line is the linear fit to the data, excluding limits (slope and error are included in each panel). A representative error bar is included in each panel.

It is important to recognize, however, that we are analysing RGB objects rather than subgiant branch stars. Therefore any conclusions we draw concerning the CNO content of subgiant branch stars in NGC 1851 will necessarily assume that the abundances we derive for RGB objects would be similar to those on the subgiant branch. That said, we can compare our average abundances for the two RGBs to measurements of subgiant branch stars by Lardo et al. (2012). They measured C and N (but not O) in subgiant branch stars in NGC 1851 and found that the fainter subgiant branch had a higher C+N content than the brighter subgiant branch, 7.64 ± 0.24 and 7.23 ± 0.31, respectively. Given that the fainter subgiant branch connects to the anomalous RGB, our C+N values for the anomalous (8.45 ± 0.14) and canonical (7.52 ± 0.21) RGBs are qualitatively consistent with Lardo et al. (2012), although we note that they used different diagnostics to measure N abundances compared to this study.

We now briefly discuss the two AGB stars. With or without the arbitrary shift in N abundance, these two objects have C+N+O values that lie between the canonical and anomalous RGB populations. As no change in the C+N+O sum is expected to take place between the RGB and AGB (e.g. see Karakas & Lattanzio 2014 and references therein), the AGBs could come from either the upper envelope of the canonical RGB C+N+O distribution or from the lower envelope of the anomalous RGB C+N+O distribution. Given the known differences in neutron-capture element abundances between the canonical and anomalous RGBs in NGC 1851 (Yong & Grundahl 2008; Villanova et al. 2010; Carretta et al. 2011), measurements of neutron-capture element abundances in the AGB stars could reveal whether they are chemically related to a particular RGB. Our Zr measurements in the canonical and anomalous RGBs follow the established pattern in this cluster, i.e. the average Zr abundance in the anomalous RGB population is 0.21 ± 0.08 dex higher than in the canonical RGB sample (see Fig. 6). Unfortunately, we could only obtain upper limits to the Zr abundance for all AGB

stars, and those limits could be consistent with either the Zr-rich anomalous RGB or the Zr-normal canonical RGB. Given the modest wavelength coverage for the NGC 1851 sample, we were unable to identify lines of neutron-capture elements that would yield reliable abundance measurements. Fig. 6 indicates that the canonical and anomalous RGBs have distinct O abundances. The two AGB stars have O abundances in accord with the anomalous RGB, although any suggestion of association would be speculation given the small numbers of stars.

As noted in the Introduction, there is evidence for a small iron abundance dispersion in NGC 1851 (Carretta et al. 2010b, 2011). For our [Fe/H] measurements, the standard deviation is 0.055 ± 0.011 dex. While Carretta et al. (2011) obtained a similar value, 0.051 ± 0.005 dex, our measurement errors are 0.08 dex (see Table 6) such that the dispersion can be explained entirely by the measurement uncertainties. In Fig. 6, there is no correlation between metallicity, [Fe/H], and C+N+O. In this figure, we also confirm the anticorrelation between O and Na (Carretta et al. 2010b, 2011). Additionally, we identify a positive correlation between Na and C+N+O.

Finally, Marino et al. (2011) examined CNO abundances in the globular cluster M22. Like NGC 1851, M22 possesses a double subgiant branch as well as a spread in *s*-process element abundances. Marino et al. (2011) found that the *s*-process rich stars (which preferentially populate the fainter subgiant branch and anomalous RGB) have a higher C+N+O content compared to the *s*-process normal stars, 7.84 ± 0.03 ($\sigma = 0.07$) and 7.57 ± 0.03 ($\sigma = 0.09$), respectively. We stress, however, that M22 and NGC 1851 are rather different objects with distinct mean metallicities, metallicity dispersions, absolute luminosities and kinematics (Dinescu et al. 1997; Casetti-Dinescu et al. 2013).

5 CONCLUDING REMARKS

We have studied the C+N+O abundance sum in the globular clusters NGC 6752 and NGC 1851. For NGC 6752, there is no evidence for an intrinsic abundance dispersion given the measurement uncertainties ($\lesssim 0.10$ dex), although the absolute value of the C+N+O sum depends on which set of molecular lines (NH versus CN) are used to obtain the N abundance. While such a result confirms previous investigations of this cluster, this study imposes considerably tighter constraints on the source of the light element abundance variations. The AGBs, fast-rotating massive stars and/or massive binaries that may have operated in the early life of this cluster to produce the abundance variations for O, Na etc. must not alter the C+N+O sum. If NGC 6752 is representative of the least complex globular clusters, then by extension all globular clusters that exhibit no evidence for a metallicity variation or multiple subgiant branches may also have a constant C+N+O abundance sum despite large variations for individual light element abundances.

For NGC 1851, we confirm a large dispersion in the C+N+O abundance sum. That is to say, the observed C+N+O dispersion ($\sigma = 0.34 \pm 0.08$ dex) far exceeds that expected from measurement uncertainties alone (~ 0.20 dex). We find that the anomalous RGB has a higher C+N+O content than the canonical RGB by a factor of ~ 0.6 dex. Such a result would support the scenario in which the two subgiant branch populations are roughly coeval, but with a different C+N+O abundance sum. Within the limited sample of canonical RGB objects, there is evidence that the C+N+O abundance dispersion exceeds the measurement uncertainties and this may indicate an intrinsic spread within this population. Confirming such an abundance dispersion within the canonical RGB popula-

tion in this cluster would be of great interest for understanding the formation history of this complicated object.

REFERENCES

Allende Prieto C., Barklem P. S., Lambert D. L., Cunha K., 2004, A&A, 420, 183
Alonso A., Arribas S., Martinez-Roger C., 1994, A&AS, 107, 365
Alonso A., Arribas S., Martínez-Roger C., 1999, A&AS, 140, 261
Asplund M., Grevesse N., Sauval A. J., Scott P., 2009, ARA&A, 47, 481
Bastian N., Lamers H. J. G. L. M., de Mink S. E., Longmore S. N., Goodwin S. P., Gieles M., 2013, MNRAS, 436, 2398
Bekki K., Freeman K. C., 2003, MNRAS, 346, L11
Bekki K., Yong D., 2012, MNRAS, 419, 2063
Blackwell D. E., Ibbetson P. A., Petford A. D., Shallis M. J., 1979a, MNRAS, 186, 633
Blackwell D. E., Petford A. D., Shallis M. J., 1979b, MNRAS, 186, 657
Blackwell D. E., Petford A. D., Shallis M. J., Simmons G. J., 1980, MNRAS, 191, 445
Blackwell D. E., Booth A. J., Haddock D. J., Petford A. D., Leggett S. K., 1986, MNRAS, 220, 549
Blackwell D. E., Lynas-Gray A. E., Smith G., 1995, A&A, 296, 217
Brown J. A., Wallerstein G., Oke J. B., 1991, AJ, 101, 1693
Buonanno R., Caloi V., Castellani V., Corsi C., Fusi Pecci F., Gratton R., 1986, A&AS, 66, 79
Campbell S. W. et al., 2012, ApJ, 761, L2
Campbell S. W. et al., 2013, Nature, 498, 198
Carpenter J. M., 2001, AJ, 121, 2851
Carretta E., Gratton R. G., Lucatello S., Bragaglia A., Bonifacio P., 2005, A&A, 433, 597
Carretta E., Bragaglia A., Gratton R., D'Orazi V., Lucatello S., 2009, A&A, 508, 695
Carretta E. et al., 2010a, ApJ, 714, L7
Carretta E. et al., 2010b, ApJ, 722, L1
Carretta E., Lucatello S., Gratton R. G., Bragaglia A., D'Orazi V., 2011, A&A, 533, A69
Carretta E., D'Orazi V., Gratton R. G., Lucatello S., 2012, A&A, 543, A117
Carretta E., D'Orazi V., Gratton R. G., Lucatello S., 2014, A&A, 563, A32
Casetti-Dinescu D. I., Girard T. M., Jílková L., van Altena W. F., Podestá F., López C. E., 2013, AJ, 146, 33
Cassisi S., Salaris M., Pietrinferni A., Piotto G., Milone A. P., Bedin L. R., Anderson J., 2008, ApJ, 672, L115
Castelli F., Kurucz R. L., 2003, in Piskunov N., Weiss W. W., Gray D. F., eds, ASP Conf. Ser. IAU Symp. 210, Modelling of Stellar Atmospheres. Astron. Soc. Pac., San Francisco, p. A20
Cohen J. G., 1981, ApJ, 247, 869
Cohen J. G., Meléndez J., 2005, AJ, 129, 303
D'Antona F., Stetson P. B., Ventura P., Milone A. P., Piotto G., Caloi V., 2009, MNRAS, 399, L151
Da Costa G. S., Held E. V., Saviane I., 2014, MNRAS, 438, 3507
de Mink S. E., Pols O. R., Langer N., Izzard R. G., 2009, A&A, 507, L1
Decressin T., Charbonnel C., Meynet G., 2007a, A&A, 475, 859

Decressin T., Meynet G., Charbonnel C., Prantzos N., Ekström S., 2007b, A&A, 464, 1029

Denisenkov P. A., Denisenkova S. N., 1990, Sov. Astron. Lett., 16, 275

Denissenkov P. A., Hartwick F. D. A., 2014, MNRAS, 437, L21

Dickens R. J., Croke B. F. W., Cannon R. D., Bell R. A., 1991, Nature, 351, 212

Dinescu D. I., Girard T. M., van Altena W. F., Mendez R. A., Lopez C. E., 1997, AJ, 114, 1014

Dotter A., 2008, ApJ, 687, L21

Dotter A., Ferguson J. W., Conroy C., Milone A. P., Marino A. F., Yong D., 2014, preprint (arXiv:1410.4570)

Fenner Y., Campbell S., Karakas A. I., Lattanzio J. C., Gibson B. K., 2004, MNRAS, 353, 789

Ferraro F. R. et al., 2009, Nature, 462, 483

Freeman K. C., 1993, in Smith G. H., Brodie J. P., eds, ASP Conf. Ser. Vol. 48, The Globular Cluster-Galaxy Connection, Astron. Soc. Pac., San Francisco, p. 608

Freeman K. C., Rodgers A. W., 1975, ApJ, 201, L71

Gratton R. G., Carretta E., Claudi R., Lucatello S., Barbieri M., 2003, A&A, 404, 187

Gratton R., Sneden C., Carretta E., 2004, ARA&A, 42, 385

Gratton R. G., Carretta E., Bragaglia A., Lucatello S., D'Orazi V., 2010, A&A, 517, A81

Gratton R. G., Carretta E., Bragaglia A., 2012a, A&AR, 20, 50

Gratton R. G. et al., 2012b, A&A, 539, A19

Gratton R. G., Villanova S., Lucatello S., Sollima A., Geisler D., Carretta E., Cassisi S., Bragaglia A., 2012c, A&A, 544, A12

Grundahl F., Catelan M., Landsman W. B., Stetson P. B., Andersen M. I., 1999, ApJ, 524, 242

Grundahl F., Briley M., Nissen P. E., Feltzing S., 2002, A&A, 385, L14

Han S.-I., Lee Y.-W., Joo S.-J., Sohn S. T., Yoon S.-J., Kim H.-S., Lee J.-W., 2009, ApJ, 707, L190

Harris W. E., 1996, AJ, 112, 1487

Ivans I. I., Sneden C., Kraft R. P., Suntzeff N. B., Smith V. V., Langer G. E., Fulbright J. P., 1999, AJ, 118, 1273

Johnson C. I., Pilachowski C. A., 2010, ApJ, 722, 1373

Joo S.-J., Lee Y.-W., 2013, ApJ, 762, 36

Kaluzny J. et al., 2013, AJ, 145, 43

Karakas A. I., Lattanzio J. C., 2014, PASA, , 31, 30

Karakas A. I., Fenner Y., Sills A., Campbell S. W., Lattanzio J. C., 2006, ApJ, 652, 1240

Kraft R. P., 1994, PASP, 106, 553

Langer G. E., Hoffman R., Sneden C., 1993, PASP, 105, 301

Lardo C. et al., 2012, A&A, 541, A141

Lee J.-W., Lee J., Kang Y.-W., Lee Y.-W., Han S.-I., Joo S.-J., Rey S.-C., Yong D., 2009, ApJ, 695, L78

Lind K., Charbonnel C., Decressin T., Primas F., Grundahl F., Asplund M., 2011, A&A, 527, A148

Marcolini A., Gibson B. K., Karakas A. I., Sánchez-Blázquez P., 2009, MNRAS, 395, 719

Marino A. F., Milone A. P., Piotto G., Villanova S., Bedin L. R., Bellini A., Renzini A., 2009, A&A, 505, 1099

Marino A. F. et al., 2011, A&A, 532, A8

Marino A. F. et al., 2012, ApJ, 746, 14

Marino A. F. et al., 2014, MNRAS, 442, 3044

Milone A. P. et al., 2008, ApJ, 673, 241

Milone A. P., Stetson P. B., Piotto G., Bedin L. R., Anderson J., Cassisi S., Salaris M., 2009, A&A, 503, 755

Milone A. P. et al., 2013, ApJ, 767, 120

Muñoz C., Geisler D., Villanova S., 2013, MNRAS, 433, 2006

Nataf D. M., Gould A. P., Pinsonneault M. H., Udalski A., 2013, ApJ, 766, 77

Norris J. E., Da Costa G. S., 1995, ApJ, 447, 680

Olszewski E. W., Saha A., Knezek P., Subramaniam A., de Boer T., Seitzer P., 2009, AJ, 138, 1570

Origlia L., Massari D., Rich R. M., Mucciarelli A., Ferraro F. R., Dalessandro E., Lanzoni B., 2013, ApJ, 779, L5

Pasquini L. et al., 2002, The Messenger, 110, 1

Prantzos N., Charbonnel C., Iliadis C., 2007, A&A, 470, 179

Ramírez I., Meléndez J., 2005, ApJ, 626, 465

Reddy B. E., Lambert D. L., Gonzalez G., Yong D., 2002, ApJ, 564, 482

Renzini A., 2013, Mem. Soc. Astron. Italiana, 84, 162

Roederer I. U., Marino A. F., Sneden C., 2011, ApJ, 742, 37

Rood R. T., Crocker D. A., 1985, in Danziger I. J., Matteucci F., Kjar K., eds, European Southern Observatory Conference and Workshop Proceedings, Vol. 21, European Southern Observatory, p. 61

Scarpa R., Marconi G., Carraro G., Falomo R., Villanova S., 2011, A&A, 525, A148

Simmerer J., Ivans I. I., Filler D., Francois P., Charbonnel C., Monier R., James G., 2013, ApJ, 764, L7

Skrutskie M. F. et al., 2006, AJ, 131, 1163

Smith G. H., 1987, PASP, 99, 67

Smith V. V., Suntzeff N. B., Cunha K., Gallino R., Busso M., Lambert D. L., Straniero O., 2000, AJ, 119, 1239

Smith V. V., Cunha K., Ivans I. I., Lattanzio J. C., Campbell S., Hinkle K. H., 2005, ApJ, 633, 392

Sneden C., 1973, ApJ, 184, 839

Sobeck J. S. et al., 2011, AJ, 141, 175

Spite M. et al., 2005, A&A, 430, 655

Stetson P. B., 1981, AJ, 86, 687

Stetson P. B., Pancino E., 2008, PASP, 120, 1332

Thompson I. B., Kaluzny J., Rucinski S. M., Krzeminski W., Pych W., Dotter A., Burley G. S., 2010, AJ, 139, 329

Ventura P., D'Antona F., 2005, ApJ, 635, L149

Ventura P., Caloi V., D'Antona F., Ferguson J., Milone A., Piotto G. P., 2009, MNRAS, 399, 934

Villanova S., Geisler D., Piotto G., 2010, ApJ, 722, L18

Yong D., Grundahl F., 2008, ApJ, 672, L29

Yong D., Grundahl F., Lambert D. L., Nissen P. E., Shetrone M. D., 2003, A&A, 402, 985

Yong D., Grundahl F., Nissen P. E., Jensen H. R., Lambert D. L., 2005, A&A, 438, 875

Yong D., Grundahl F., Johnson J. A., Asplund M., 2008a, ApJ, 684, 1159

Yong D., Meléndez J., Cunha K., Karakas A. I., Norris J. E., Smith V. V., 2008b, ApJ, 689, 1020

Yong D., Grundahl F., D'Antona F., Karakas A. I., Lattanzio J. C., Norris J. E., 2009, ApJ, 695, L62

Yong D. et al., 2013, MNRAS, 434, 3542

Yong D. et al., 2014, MNRAS, 441, 3396

Zoccali M., Pancino E., Catelan M., Hempel M., Rejkuba M., Carrera R., 2009, ApJ, 697, L22

SUPPORTING INFORMATION

Additional Supporting Information may be found in the online version of this article:

Table 4. Line list for the NGC 1851 stars (http://mnras.oxfordjournals.org/lookup/suppl/doi:10.1093/mnras/stu2334/-/DC1).

Please note: Oxford University Press are not responsible for the content or functionality of any supporting materials supplied by the authors. Any queries (other than missing material) should be directed to the corresponding author for the article.

This paper has been typeset from a TEX/LATEX file prepared by the author.